JOURNAL OF MATERIALS SCIENCE: MATERIALS IN MEDICINE 5 (1994) 113–118

The effect of microstructural features on the biaxial flexural strength of leucite reinforced glass-ceramics

M. Y. SHAREEF, R. VAN NOORT, P. F. MESSER*
*Department of Restorative Dentistry and *Department of Engineering Materials, University of Sheffield, Western Bank, Sheffield S10 2SZ, UK*

V. PIDDOCK
Biomaterials Science Unit, University Dental Hospital of Manchester, Higher Cambridge Street, Manchester M15 6FH, UK

In this study the effect of size and distribution of leucite crystals on the biaxial flexural strength of five leucite reinforced glass-ceramics used in dentistry for the construction of veneers was investigated. Three of these were found to have a non-uniform distribution of leucite crystals, which were associated with a considerable degree of microcracking in the glassy matrix around the leucite crystals. The mean values of biaxial flexural strength of these ceramics ranged from 56 to 70 MPa. The other two ceramics exhibited a more uniform distribution in their leucite crystals, which were also finer in size. The latter ceramics had a significantly higher biaxial flexural strength which ranged from 120 to 137 MPa. When the particle size of the starting powders of the three low strength ceramics was reduced, a more uniform microstructure with less evidence of microcracking was produced in the fired ceramics and the biaxial flexural strength values were significantly increased. We conclude that uniformity of microstructure and leucite crystal size are major factors in determining the biaxial flexural strength of leucite reinforced glass-ceramics.

1. Introduction

The desirability of a more conservative approach to tooth preparation coupled with an increased demand for aesthetic dentistry have led to the recent rise in popularity of porcelain and other ceramic veneers. Ceramic restorations provide both durable aesthetic appeal and excellent biocompatibility. However, ceramics in general are prone to mechanical failure in tension because, unlike more ductile metal restorations, they are unable to accommodate tensile strain by plastic deformation. Furthermore, the fabrication of procelain restorations inevitably leads to the incorporation of voids which function as stress raisers. The presence of porosity in porcelains crowns has been observed previously [1], although porosity in thin porcelain veneers has not been studied.

In addition, the behavioural properties of dental porcelains will depend on other microstructural features. In particular the constituent phases will be important. For example, crystalline phases may act as crack stoppers, effectively increasing fracture toughness. Piddock *et al.* [2] have used back scattered electron microscopy to resolve phases present in some aluminous jacket crown porcelains, and have highlighted the complexity of the microstructures in such materials.

The presence of different phases may result from the use of physical mixtures of glass powders [2]. In addition, phase separation may occur during thermal processing in the dental laboratory, with the introduction of new phases or growth of existing crystalline regions. Whilst the inclusion of phases of differing refractive index is believed to be beneficial in terms of light scattering within the porcelain [3], problems may ensue due to incompatibility of thermal expansion of the various phases present.

Compositional ranges for dental porcelains have been widely reported [3, 4], but less is known about the detailed microstructure of the individual phases present in dental porcelains. Procelain veneers and inlays have been fabricated from both porcelain jacket crown and metal bonded porcelains as well as materials designed specifically for the production of such restorations. The microstructural features of the latter class of procelains have not been reported on hitherto and it was the aim of this study to learn more of the characteristics of the porcelain powders and the microstructural features of the fired veneer porcelains in order to assist future optimisation of their mechanical properties.

2. Materials and methods

Five commercial dental ceramics, which are detailed in Table I, were used in this study. The particle size distribution of the starting and modified powders were

0957–4530

TABLE I Details of dental ceramics used in the study

Materials	Code	Shade No.	Batch No.	Manufacturer
Mirage	MI	Body D-4	8130	Myron Int. Inc. Kansas, USA
Chameleon	CH	Body D-4	059020	Myron Int. Inc. Kansas, USA
Flexoceram	FL	D-EB1	442	Elephant Ceramics, Hoorn, Netherlands
G-Cera	GC	DB1	150501	GC Int. Corporation, Tokyo, Japan
Optic-HSP	OP	A2	070603	Jeneric, Conn., USA

determined using a particle size analyser. The microstructural features of the fired ceramics were examined using back scattering imaging (BSI) and scanning electron microscopy (SEM) and their biaxial flexural strengths were measured.

2.1. Sample preparation

Refractory moulds of Flexoceram (Elephant Ceramics, Hoorn, Holland) were produced using the manufacturers' recommended procedures. Each mould contained six wells measuring 12 mm in diameter and 3 mm in depth. A mixture of ceramic powder and condenser liquid (Myron Inc., Kansas, USA) was cast into the refractory mould and vibrated to condense the particles and subsequently fired according to the manufacturers' instructions appropriate to each ceramic. The fired discs were ground with 600 grit SiC paper (Buehler-Met, Metallographic Grinding Paper, UK) to produce flat parallel surfaces and their thickness was measured by a micrometer.

A problem encountered with many of the samples was extensive cracking of the discs after firing. It was thought that this was due to the penetration of the ceramic powder into the pores of the refractory mould surface, creating a mechanical bond between the two materials thus preventing the ceramic from shrinking freely on firing. To avoid this problem a thin layer of sodium alginate separator (Metrocry, Plaster Coating Solution, Metrodent Ltd. UK) was painted on the walls of the refractory moulds prior to condensing the ceramic and this resolved the problem.

2.2. Particle size analysis

Particle size distributions of the ceramic powders were determined using a Coulter LS130 Particle Size Analyser System, which employs a laser diffraction method. The powders were placed in distilled water and stirred continuously to aid dispersion of the fine particles. A few drops of a filtered solution 2 wt % Calgon (sodium hexameta phosphate) in distilled water were added as a deflocculant.

The particle size of MI, FL and CH powders were reduced using a milling process. A suspension containing ≈ 18 vol % of the powder in distilled water and few drops of Calgon (sodium hexameta phosphate) was prepared. This suspension was mixed in a cylindrical plastic pot 75 mm diameter and 140 mm long containing 35 zirconia balls, 12.5 mm diameter. The pot was rotated on rollers at 75 rev/min for approximately 20 h to break down the coarser particles size.

2.3. Scanning electron microscopy

The microstructure of polished sections of the fired compacts were examined after either carbon coated for BSI or gold coated for SEM. The polished sections were prepared by vacuum impregnating the compacts with epoxy resin, followed by grinding and polishing with SiC paper and diamond pastes down to 1 μm. Etching with 1% hydrofluoric acid (HF) for 30 s was carried out on some samples to expose the structure of the crystalline phase in these ceramics.

2.4. Biaxial flexural strength measurements

The biaxial flexural strength values for ten discs of each material were determined by using the equation reported by piddock *et al.* [4] at a crosshead speed of 0.5 mm min^{-1} (Lloyd M5K). Assuming a Poisson's ratio of porcelain of 0.25, the simple form of this equation is:

$$\sigma_{max} = P/h^2 \{0.606 \log_e(a/h) + 1.13\}$$

where σ_{max} is the maximum biaxial flexural strength, P is the load to cause fracture, a is the radius of the knife-edge support and h is the sample thickness.

3. Results and discussion

The particle size distribution of two of the starting powders are presented in Fig. 1. The distribution for MI is typical of all the other powders except GC. The results show that the powders consist of a bi- and tri-modal particle size distribution, presumably to enhance the packing density of the green body and thus minimise shrinkage on drying and firing. The mean and maximum particle size for the powders are shown in Table II. Again, the mean particle size is similar for all ceramic powders except for the GC powder which has a larger mean particle size and corresponding larger maximum particle size. SEM examination of the starting powders effectively confirmed the particle size analysis. Fig. 2a and b shows examples of MI and GC powders at the same magnification with the GC powder clearly being coarser and also shows the irregular nature of the particles.

BSI micrographs of the microstructures of the fired ceramics are presented in Fig. 3a–e. The microstructure of MI (Fig. 3a) suggests that there is phase

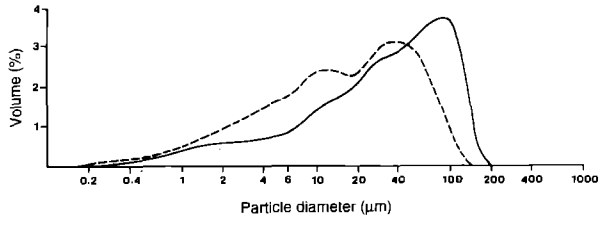

Figure 1 Particle size distribution of as-received ceramic powders for MI (– – –) and GC (———).

TABLE II The mean, maximum particle size distribution and standard deviations for the five starting powders, calculated for a range of 0.1 μm to 900 μm

Materials	Mean (μm)	SD (±)	Approx. maximum size (μm)
MI	26.02	25.24	130
CH	25.15	27.65	130
FL	28.76	24.66	110
GC	47.39	37.87	190
OP	28.52	25.03	130

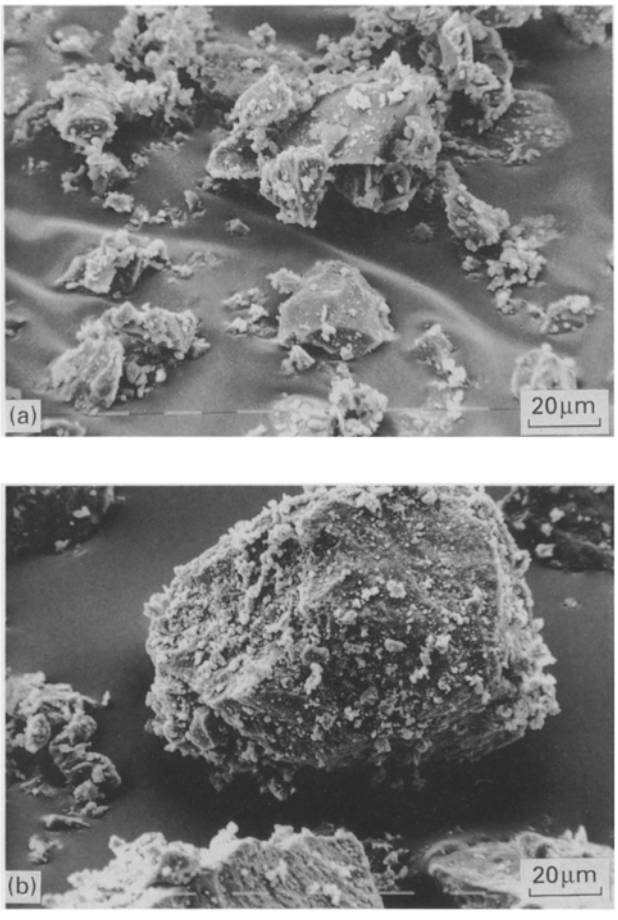

Figure 2 SEM micrographs of (a) MI ceramic powder showing the angulated morphology and (b) GC ceramic powder showing the large size of the particles.

separation in the glass matrix as indicated by the lighter and darker regions, which was not so evident in the other ceramics. In MI, the leucite appears as individual crystals of the order of 5 to 10 μm, randomly and non-uniformly distributed throughout the glassy matrix. For CH and FL (Fig. 3b and 3c, respectively) the leucite is present as clusters of approximately 30 μm diameter. Each cluster consists of numerous smaller crystals. In FL these clusters, which have a distinctly dendritic appearance, are particularly difficult to differentiate using BSI.

Microcracks associated with large clusters of leucite crystals are readily observed in CH and FL. The microstructures of GC and OP (Fig. 3d and 3e, respectively) show a considerably more uniform distribution of leucite crystals, with no evidence of the microcracking, so readily apparent in Fig. 3a, 3b and 3c for MI, CH and FL, respectively. Using the 1% HF etching process, the leucite crystals are readily identifiable by their distinctive surface pattern when examined under the scanning electron microscope (Fig. 4). The crystals consist of lenticular plates, giving them a striped appearance as previously described by Barreiro *et al*. [5]. For MI the individual crystals (Fig. 4a) and for CH and FL (Fig. 4b and 4c) the clusters of leucite with their dendritic network structure are more readily seen than from the back scattered images.

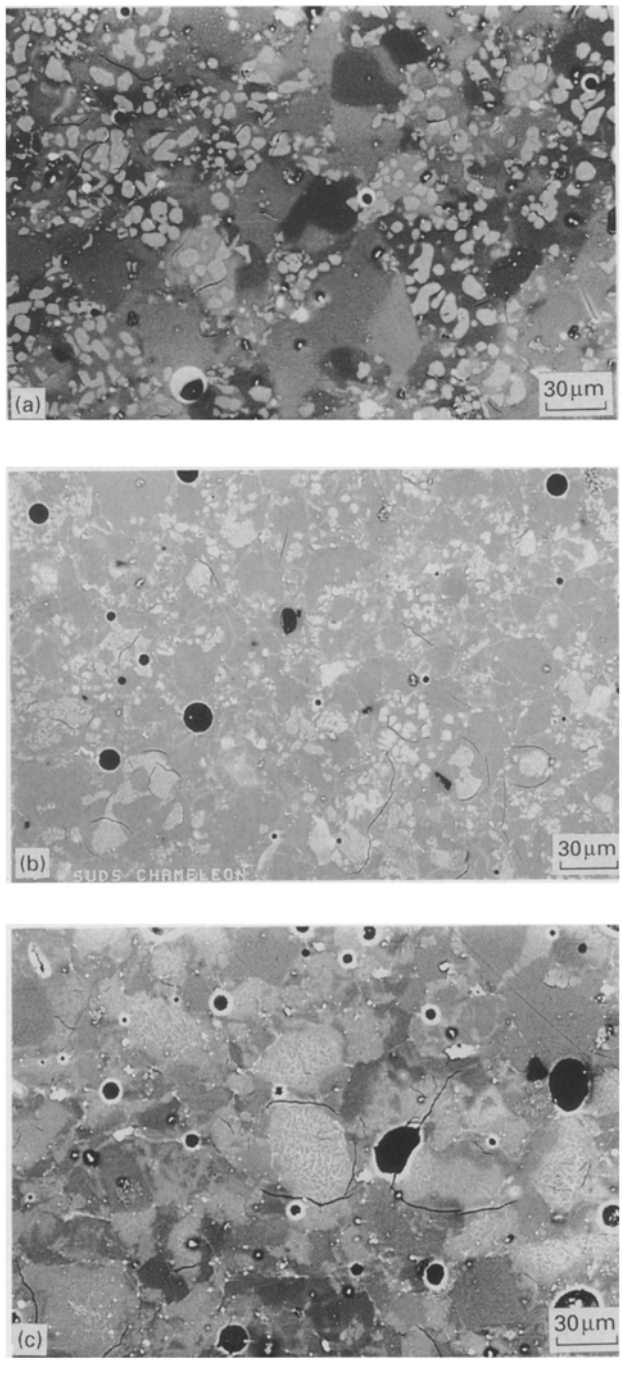

Figure 3 Back scattered image micrographs of: (a) MI showing phase separation in the glassy matrix as indicated by the different shades of grey. The light coloured particles are leucite crystals; (b) CH showing extensive cracking around the crystalline phase; (c) FL with clear indication of microcracking around the crystalline phase; (d) GC showing a uniform distribution of leucite crystals; (e) OP showing a uniform distribution of leucite crystals.

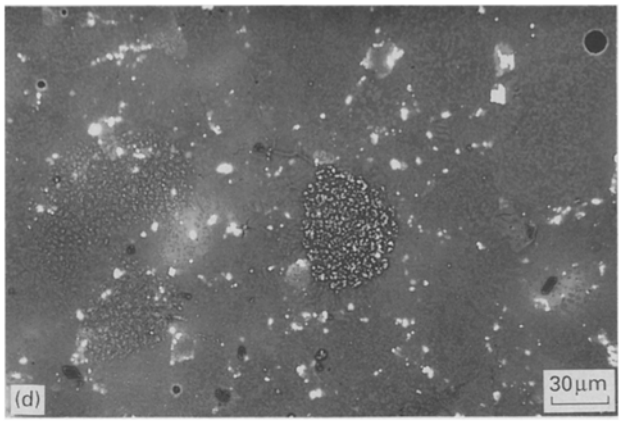

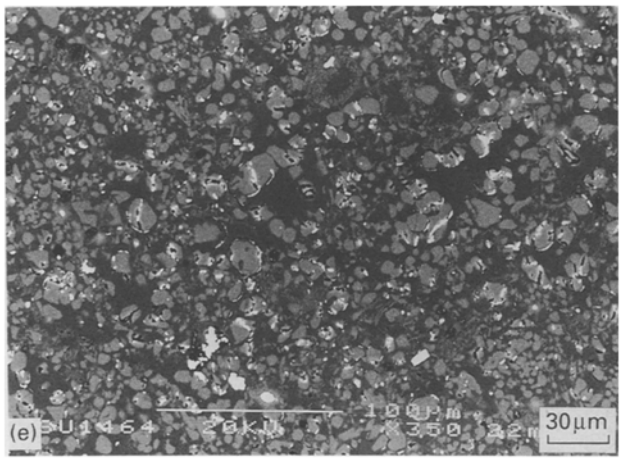

Figure 3 Continued

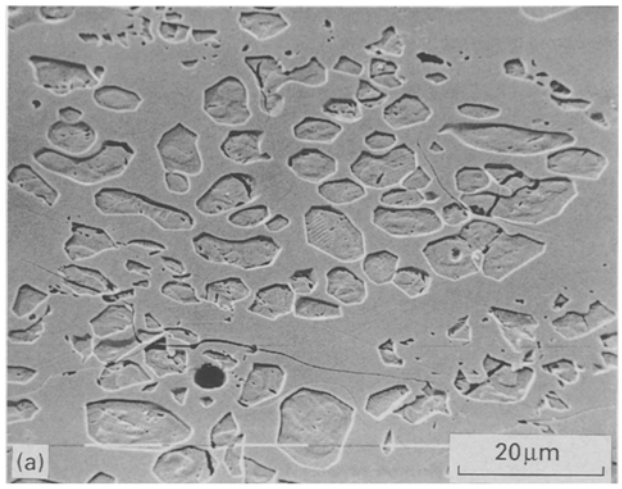

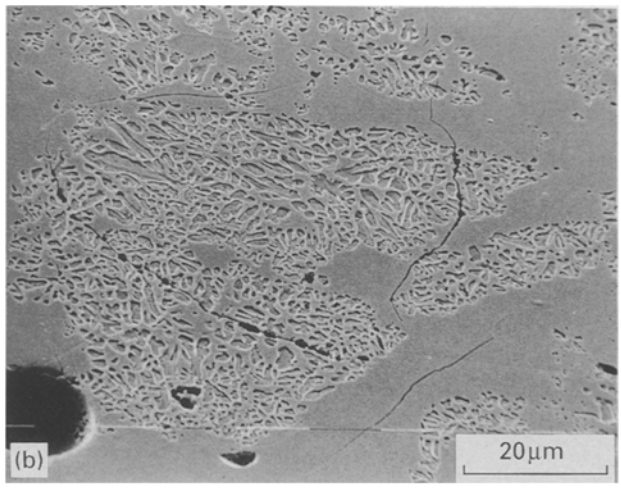

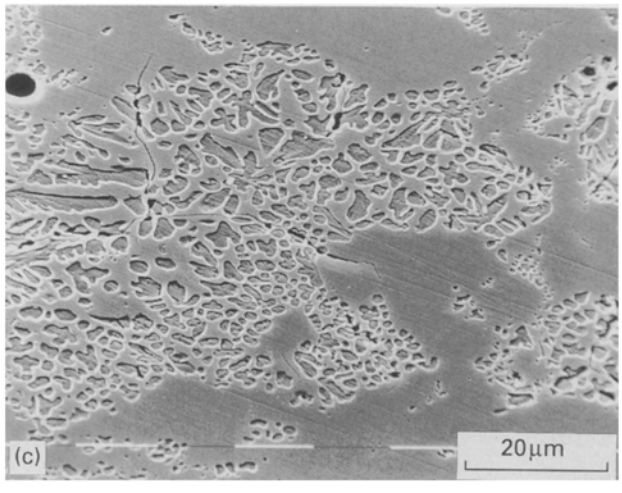

Figure 4 SEM micrographs of the appearance of clusters of leucite crystals exposed by light etching with 1% HF for 30 s (a) MI, (b) CH and (c) FL.

Microcracking in the glass matrix, either around the individual crystals as in MI or around the clusters in CH is again clearly evident. There is also evidence of microcracking within the leucite crystals and in some instances cracks run from the glassy matrix into and through the leucite crystals. The etched appearance of GC and OP are quite different in that there is a much more uniform distribution of the leucite crystals as shown in Fig. 5 for GC ceramic. Although there are small cracks within the leucite crystals, these do not extend into the glass matrix.

The presence of microcracks around the clusters of leucite crystals suggests that non-uniform shrinkage of the glassy matrix and crystalline phases had occurred on cooling due to differences in their thermal expansion behaviour and the cubic to tetragonal leucite transformation of leucite [6]. These microcracks can also occur around individual leucite crystals but only when these are exceptionally large [7]. These microcracks, combined with the non-uniform distribution of the crystalline phase, will severely limit the mechanical properties of these materials because they increase the inherent flaw size and may act as fracture-initiating flaws [8], increasing the chances of catastrophic crack propagation. These flaws depend upon the size of the starting particles and the distribution of the crystalline phase in the fired ceramics.

The mean biaxial flexural strengths, standard deviations and coefficients of variation are given in Table III. There is a significant difference between the mean values of biaxial flexural strength of MI, CH, FL on the one hand and on the other of GC, OP. This is related to the non-uniformity of the microstructure and the presence of the microcracks around the large leucite crystals in the former ceramics. In addition, both GC and OP appear to have a denser distribution of leucite crystals when compared with the other three ceramics, which will contribute to a higher biaxial flexural strength [10].

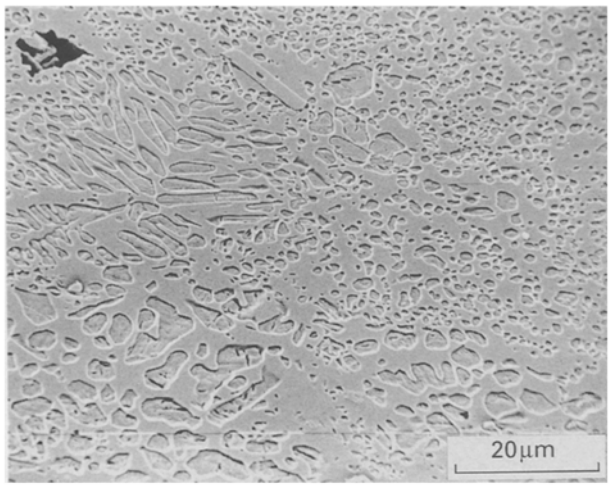

Figure 5 SEM micrograph of GC showing a uniform distribution of leucite crystals exposed by etching with 1% HF for 30 s.

TABLE III The mean values of biaxial flexural strength, standard deviations and coefficients of variation of dental ceramics used in this study

Materials	Mean(MPa)	SD (±)	%CV
MI	70	6	8.6
CH	56	5	8.9
FL	62	7	11.3
GC	119	15	12.6
OP	137	11	8.0

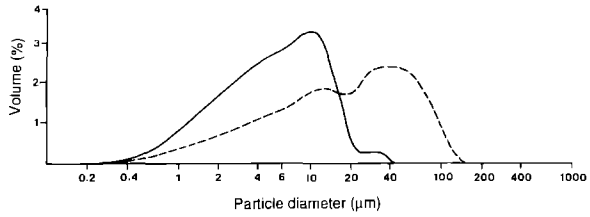

Figure 6 Comparison of the particle size distribution of the as-received (– – – –) and milled (——) MI powder.

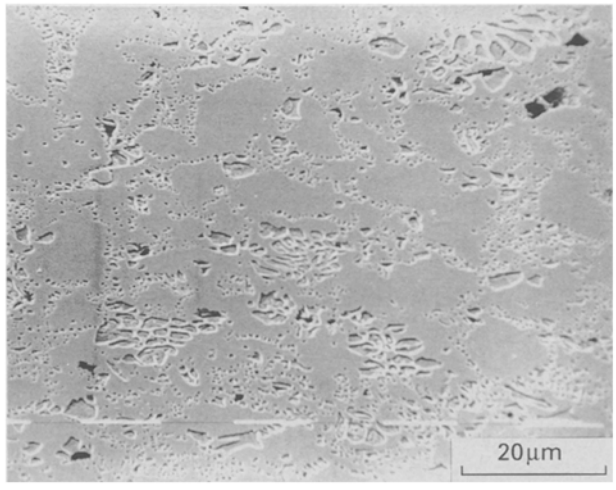

Figure 7 SEM micrograph of the milled ceramic of MI, exposed by light etching with 1% HF for 30 s.

TABLE IV The mean values of biaxial flexural strength, standard deviation and coefficients of variation for modified ceramics

Materials	Mean (MPa)	SD (±)	%CV
MI	120	15	12.5
CH	96	12	12.5
FL	82	14	17.1

The properties of a ceramic can be seen in terms of its characteristic properties and behavioural properties. The behavioural properties, such as tensile strength, fracture toughness and thermal expansion coefficient, depend on the starting material, the production of the green body and the firing process (i.e. behavioural properties depend on characteristic properties). These behavioural properties describe how the material or fired product behaves when subjected to changing conditions. The characteristics properties would be considered as constitutional and the structural characteristics [9]. For example, the characteristics properties of a green ceramics, which determine whether it will shrink uniformly during firing, are such factors as porosity, composition, and particle size. To behave in a uniform way on a given scale of size during a processing operation, a material must have uniform characteristic properties at the start of the operation on the scale of size being considered and the treatment given during the operation, must be uniform. Therefore, to achieve a uniform microstructure on the scale of size related to the average size of leucite particles, the starting powders of MI, CH and FL were reduced using a ball milling process. Fig. 6 shows an example of the particle size distribution for both the starting and modified powders of MI. Using 1% HF, the etched microstructure of the modified ceramics was examined using SEM as shown in the example for MI in Fig. 7. The fired microstructure of the modified ceramic showed a more uniform distribution of the leucite crystals with respect to the characteristics properties on a scale of size related to the leucite particles and less evidence of microcracking. In the case of MI, shown in Fig. 7, there is no evidence of microcracking of the glassy matrix, although there is still some microcracking within the leucite crystals. As a consequence of these changes to the microstructural features, the biaxial flexural strength of MI was increased from 70 to 120 MPa, a 70% improvement. A similar improvement in biaxial flexural strength was achieved for CH, although for FL only a 30% improvement could be obtained. The detailed results are presented in Table IV. A biaxial flexural strength for MI was obtained which is comparable to that of GC and OP.

Given that the microstructural information suggests that the three low-strength ceramics contain considerably less leucite than GC or OP, this would indicate that there is still further potential to increase the strength of these ceramics by raising the leucite content. This may be a more worthwhile route to explore than simply milling the starting powders. The problem with the milling processing route is that it

results in a considerable increase in firing shrinkage and opacity, which are undesirable side effects for dental ceramics. Therefore, considerably more work is needed to understand the effects of compositional and processing factors on the microstructure and properties of this class of dental ceramics in order to optimise their mechanical properties.

4. Conclusions

1. The ceramic powders MI, CH, FL and OP have a similar particle size, whereas GC has a coarser particle size distribution.

2. A leucite crystalline phase was present in all the ceramics, consisting of dendritic clusters of tiny crystals in case of CH, FL and GC and larger individual crystals in MI, OP.

3. Extensive microcracking was observed in the glass matrix around and within the leucite phase of MI, CH and FL. GC and OP showed only minimal evidence of microcracking, which was always present within the leucite crystals.

4. MI, CH and FL had a significantly lower biaxial flexural strength than GC and OP.

5. Ball milling of MI, CH and FL significantly increased their biaxial flexural strength.

References

1. P. M. MARQUIS, J. WILLIAMS, V. PIDDOCK and H. J. WILSON, *Quint. Dent. Technol.* **10** (1989) 173.
2. V. PIDDOCK, P. M. MARQUIS and H. J. WILSON, *Br. Dent. J.* **156** (1984) 395.
3. J. W. McLEAN "The science and art of dental ceramics", Vol I (Quintessence Publishing Co., Chicago, 1980).
4. P. M. MARQUIS, *Metals Mater.* **5** (1989) 145.
5. M. M. BARREIRO, O. RIESGO and E. E. VICENTE, *Dent. Mater.* **5** (1989) 51.
6. J. R. MACKERT, Jr. in Proceeding of the 4th International Symposium on Ceramics, Chicago, III, 1985, edited by J. D. Preston (Quintessence Publishing Co., Chicago, 1988) p. 53.
7. C. W. FAIRHURST, P. E. LOCKWOOD, R. D. RINGLE and W. O. THOMPSON, *Dent. Mater.* **8** (1992) 203.
8. D. W. JONES and H. J. WILSON, *J. Oral. Rehab.* **2** (1975) 379.
9. M. Y. SHAREEF, Ph.D. thesis, University of Sheffield, Sheffield (1991).
10. R. R. SEGHI, T. DAHER and A. CAPUTO, *Dent. Mater.* **6** (1990) 181.

Received 4 August
and accepted 14 September 1993